Astronomy
&
Astrophysics

Compositional dependence of infrared absorption spectra of crystalline silicates

I. Mg–Fe pyroxenes

H. Chihara[1,2], C. Koike[2], A. Tsuchiyama[1], S. Tachibana[3], and D. Sakamoto[1]

[1] Department of Earth and Space Science, Osaka University, 1-1, Machikaneyama, Toyonaka, Osaka 560-0043, Japan
[2] Laboratory of Physics, Kyoto Pharmaceutical University, Misasagi, Yamashina, Kyoto 607-8414, Japan
[3] Department of Geological Sciences, Arizona State University, Tempe, AZ 85287-1404, USA

Abstract. Crystalline Mg–Fe pyroxenes with different Mg/(Mg + Fe) ratio ($MgSiO_3$ ~ $Mg_{0.5}Fe_{0.5}SiO_3$ and $FeSiO_3$) were synthesized in laboratory and their absorption properties were investigated in the infrared region. The absorption spectrum of ferrosilite ($FeSiO_3$) is reported for the first time in this work. Our study confirmed that the Mg end members have sharp and characteristic features in the far-IR region and in particular that it is easy to distinguish the two types of crystalline structures (orthorhombic and monoclinic) in this wavelength range. In addition we find that the absorption spectra depend on the chemistry and crystal structure of the material: (1) The far-IR features which are prominent in the Mg end members, vanish when the iron concentration is increased. However, even in the iron bearing pyroxenes, the variation of the mid-IR features with Fe concentration is less significant in comparison to that of the far-IR features. (2) Peak positions shifted to longer wavelength an increase in iron concentration; the dependence of the shift is approximately linear in wavenumber (cm^{-1}). (3) Bandwidths of the far–IR bands for the end members are significantly smaller than those of solid solutions. These results suggest that the far-IR features of pyroxenes are very sensitive to chemical composition and crystal structure. Therefore, far-IR features are a very useful constraint on the chemical composition and crystal structure of circumstellar pyroxenes.

Key words. circumstellar matter – line: profiles – infrared: ISM: lines and bands – methods: laboratory – ISM: dust, extinction

1. Introduction

Following the ISO (Infrared Space Observatory) mission, crystalline solid materials were found to exist in circumstellar environments as well as solar system objects (Waters et al. 1996; Waelkens et al. 1996; Whittet et al. 1996, etc.). Laboratory spectroscopic studies of circumstellar dust candidates are required to understand not only observational data correctly but also the physical properties of circumstellar environments. The existence of crystalline silicates such as olivine, $(Mg \cdot Fe)_2SiO_4$ and Mg–Fe pyroxene, $(Mg \cdot Fe)SiO_3$ in circumstellar dust shell of oxygen rich evolved and young stars, are considered particularly important. Therefore, optical properties of these minerals have been studied extensively in recent years (Jäger et al. 1998; Koike et al. 2000, etc.) These mineral species are formed as perfect solid solutions of magnesian and ferrous end members within certain stoichiometric ratios, namely divalent cation (Mg and Fe) : Si = 2 : 1 and 1 : 1 for olivine and pyroxene,

respectively. The simplest approach is that the Mg/(Mg+Fe) ratio of the dust grain is dependent on the chemical composition of the gas from which the grain are condensed. However, it is reported that almost identified absorption bands from ISO observations are attributed to the mineral species with the chemical compositions extreamly close to the Mg end member. The depletion of iron in circumstellar crystalline silicates was explained qualitatively within a framework of thermodynamic equilibrium condensation theory by Tielens et al. (1998). Rietmeijer et al. (1999) also tried to resolve the issue by an experimental study of gas-to-solid condensation in a Mg-Fe-SiO-H_2-O_2 vapor. As a result, they concluded that ferromagnesiosilica grain will not form as primary condensates in circumstellar outflow.

The spectral variation of olivine depending on its chemical composition was first investigated by Koike et al. (1993). They reported that absorption bands shifted longer wavelength as with increasing iron concentration, based on measurements of natural and synthetic olivines of which the chemical composition ranged from forsterite (Mg_2SiO_4) to $Mg_{0.8}Fe_{1.2}SiO_4$.

Jäger et al. (1998) also reported that similar tendency of the band shift on their investigations for four olivine samples which compositions are ranged between the Mg and Fe end members. As for the olivines, optical data of pyroxenes is very important. However, to our knowledge the only compositional study on pyroxenes in the astrophysical literature is that by Jäger et al. (1998) who measured absorption spectra of a synthesized clinoenstatite and three natural orthopyroxenxes of which the chemical composition correspond to enstatite to hypersthene. However, unfortunately their natural samples were contaminated with weathering alteration products such as talc and metal oxides as well as minor elements such as Ca, Al, Ti and Mn etc. Indeed, it is natural that the cosmic dust grain in circumstellar environment have diversity of chemical composition in their minor elemental components as well as their major components. It is possible that circumstellar grains are altered by some physical processes (e.g. hydration, annealing etc.) and contaminated by some impurities. The advantage of measuring synthetic samples with simple chemical compositions is that the spectral properties depend only on the major chemical composition. Therefore, in order to improve on the results of Jäger et al. and to resolve the compositional dependence of optical properties precisely, we tried to newly synthesize crystalline pyroxenes in a wide compositional range ($MgSiO_3 \sim Mg_{0.5}Fe_{0.5}SiO_3$ and $FeSiO_3$), and measured the absorption spectra in the mid- and the far-infrared regions.

2. Sample preparations and measurements

The chemical formula of Mg–Fe pyroxene is $[Mg_x, Fe_{1-x}]SiO_3$, ($0 \leq x \leq 1$). The Mg end member ($x = 1$) is called enstatite (En), while the Fe end member ($x = 0$) is ferrosilite (Fs). Hereafter, following the conventional description, the chemical composition of $[Mg_x, Fe_{1-x}]SiO_3$ is described as En_X, where X is the mole percentage of the enstatite component ($X = 100\,x$).

In this work, pyroxene crystals of En_{100} (orthoenstatite; Oen, and clinoenstatite; Cen), En_{90}, En_{80}, En_{70}, En_{60}, En_{50} and ferrosilite (Fs) were synthesized. Chemical compositions and crystal systems of the synthesized samples are listed in Table 1.

The orthoenstatite (Oen) single crystal was synthesized with the flux method (Tachibana 2000), and the clinoenstatite (Cen) was obtained by annealing the orthoenstatite at 1200 °C for 9 hours in the atmosphere. For the synthesis of Mg–Fe pyroxenes, MgO, FeO and SiO_2 powders were mixed in appropriate mole ratios. The MgO and the SiO_2 powders were reagent grade chemicals and the FeO powders were prepared from reagent grade ferric oxalate ($FeC_2O_4 \cdot 2H_2O$) by heating at 900 °C in a controlled H_2–CO_2 gas flow for about 12 hours. O_2 fugacity was at about 0.5 log-unit below the MW(Magnetite–Wüstite) buffer curve, the value corresponded to about 3×10^{-11} atm. In the domain beneath the MW–buffer curve and above the IW(Iron–Wüstite) buffer curve, equilibrium between Fe^{2+} and Fe^{3+} is achieved (e.g., Wood et al. 1990). The value in this study was somewhat higher than that of usual experiments on planetary material. However, as far as ferric oxalate is used as a starting material, in which Fe^{3+} does not exist, Fe^{2+} is stable at the value. Therefore, O_2 fugacity could be considered as sufficiently controlled. These mixtures

Table 1. Properties of synthesized samples.

sample	nominal composition	analytical composition	crystal structure
Oen	$MgSiO_3$	–	ortho
Cen	$MgSiO_3$	–	clino
En_{90}	$Mg_{0.90}Fe_{0.10}SiO_3$	$Mg_{0.91}Fe_{0.08}SiO_3$	clino
En_{80}	$Mg_{0.80}Fe_{0.20}SiO_3$	$Mg_{0.82}Fe_{0.18}SiO_3$	ortho
En_{70}	$Mg_{0.70}Fe_{0.30}SiO_3$	$Mg_{0.72}Fe_{0.28}SiO_3$	ortho
En_{60}	$Mg_{0.60}Fe_{0.40}SiO_3$	$Mg_{0.63}Fe_{0.36}SiO_3$	ortho
En_{50}	$Mg_{0.50}Fe_{0.50}SiO_3$	$Mg_{0.52}Fe_{0.48}SiO_3$	ortho
Fs	$FeSiO_3$	–	ortho

were pressed into pellets with 5 mm radius and 2 ∼ 3 mm thick. These pellets were hung by platinum wire and then heated in a furnace at 1200 °C for 96 hours at atmospheric pressure. O_2 fugacity was controlled by H_2–CO_2 gas flow as before. The products were a sintered aggregation of polycrystalline pyroxene.

Careful observation of the products under an SEM (secondary electron image microscope) with back scattered electron images showed that any phase other than pyroxene and heterogeneity in pyroxene were not detected. Chemical compositions were analyzed by an electron probe micro analyzer (EPMA, JEOL-733) at Osaka University. The accelerating voltage was 15 keV and sample current was 1.2 nA. As a results, the Mg/(Mg+Fe) ratios of the products were almost consistent with nominal ratios. Phase diagram of the system $MgSiO_3$–$FeSiO_3$ at 1 atm (Huebner 1980) indicates that the crystalline phase of En_{90} and En_{80}–En_{60} at 1200 °C is protopyroxene and orthopyroxene, respectively. Although, the phase of the En_{50} is indicated as a mixture of olivine and pigeonite at 1200 °C, both of the electron micro probe and X-ray diffraction analyses showed that the product was orthopyroxene. We also tried to synthesize En_{40}, but failed because phase separation occurred and pyroxene phases were not produced. As mentioned by Jäger et al. (1998), synthesizing pyroxenes becomes more difficult when the iron concentration increases. Indeed, the pyroxene phase diagram shows that the phases of pyroxene are very complex especially in the compositional region from En_{40} to Fs. Therefore, obtaining a single crystalline phase of such Fe–rich pyroxenes seems to be difficult at atmospheric pressure.

The Fe end member (ferrosilite) is unstable at atmospheric pressure and room temperature. Therefore, it cannot exist naturally on the Earth's surface in general, and probably it cannot be condensed directly from gas in circumstellar environment, either. However, ferrosilite can be produced at high pressure. In this work, orthoferrosilite was synthesized by use of a multi-anvil press (Kobelco DIA-6 at Osaka University). First of all, polycrystalline Fe_2SiO_4 were synthesized at atmospheric pressure from the mixture of SiO_2 and FeO powder with the same method mentioned above. Then, the mixture of the produced Fe_2SiO_4 and SiO_2 with appropriate mole ratio were put into a gold capsule and pressed at 4 GPa, and then heated at 1000 °C for 1 hours. The obtained synthesized orthoferrosilite was polycrystalline powder sized less than 10 μm. In the produced Fs, very small amount of SiO_2(< 0.5%) was detected by EPMA

and SEM-imaging analyses. This is perhaps residual quartz escaped from chemical reaction. However, this amount of impurity does not affect the spectra.

To prepare the absorption measurements, the samples were crushed and ground in an agate mortar for about 1 hour until the grains were approximately less than 1 μm in size. These fine powders were dispersed and embedded in appropriate matrix; KBr for the mid–IR measurements (1600–300 cm^{-1}) or polyethylene for the far–IR measurements (650–50 cm^{-1}). The measurements were performed by Nicolet Nexus 670 FT–IR spectrometer (Kyoto Pharmaceutical Univeristy) at room temperature. The measured wavenumber range was 1600–50 cm^{-1}. The resolutions of the measurements were 1.0 cm^{-1} in the mid-IR region (1600–300 cm^{-1}) for all samples. In the far-IR region (300–50 cm^{-1}), the lower resolutions were used (4.0 cm^{-1} for Fs–En$_{90}$, and 2.0 cm^{-1} for the Mg end members) to avoid interference fringe.

3. Results

The mass absorption coefficients; κ(cm^2/g) of the samples are plotted in Fig. 1. As a whole, the spectral feature of pyroxenes are very complex. The uppermost spectrum is orthoferrosilite (Fs). Below Fs the Mg/(Mg+Fe) ratio increases from ~50% in En$_{50}$ to 100% in En$_{100}$ in increments of 10% for subsequent spectra. The crystal structures of En$_{100}$(Cen) and En$_{90}$ were monoclinic, other samples were orthorhombic. For the Mg end members, the features were consistent with our previous measurements (Koike et al. 2000; Chihara et al. 2001).

Peak positions of all samples in μm are listed in Table 2. With the exception of En$_{90}$ (which may contain some forsterite impurities) the spectral variation with the chemical composition is almost continuous. Some absorption bands newly appeared and/or disappeared especially near the chemical composition close to the Mg and the Fe end members. In En$_{90}$, some small absorption bands appeared at 12.9 and 16.5 μm which are probably due to forsterite, although the chemical and SEM-image analyses did not show any inhomogeneity and phase separation.

3.1. Distinction between clino- and orthoenstatite in the far–IR region

The two crystal structures of enstatite (Oen and Cen) show almost same spectral features in the mid–IR region up to about 40 μm. While in the far–IR region, they can be distinguished easily, because both enstatites have small but sharp and characteristic features in this region, such as two double bands at around 50 and 70 μm of orthoenstatite, and a single band at 66 μm of clinoenstatite. Although, these far–IR characteristic features of the Mg end members are very sharp and prominent, En$_{90}$ does not exhibit these features clearly.

In the spectrum of En$_{90}$, the 67 μm band of clinoenstatite vanished, and the triple bands at around 43 μm turned to a double structure. While, on the spectrum of En$_{80}$, both of the double structures of the band at around 50 μm and 70 μm of orthoenstatite disappeared completely. Instead, a small shoulder

around 70 μm began to appear. This 70 μm shoulder become clearer as a single band from about En$_{60}$, and shifted with the iron concentration to 86 μm on Fs. In the mid–IR region the variations in absorption feature with crystal structure were less distinct than those in the far–IR region.

3.2. Band shifts as a function of Mg/(Mg+Fe) ratio

Figure 2 shows the peak positions of absorption bands as a function of their chemical compositions. The horizontal axis indicates the band position in wavenumbers (cm^{-1}) and the vertical axis indicates the enstatite content (%). The size of the plotting symbols indicate the approximate intensity of the band: solid circles represent the position of a peak, empty circles indicate a shoulder. Most of the absorption bands are systematically shifted to longer wavelengths with an increase in the iron concentration. In wavenumbers the relationship the shift with changing Fe concentration is approximately linear. The most significant shift in frequency is for the 43 micron peak of Cen and Oen which moves from about 43 μm (233 cm^{-1}) on En$_{100}$ to 56 μm (179 cm^{-1}) on Fs.

These results are consistent with those of Jäger et al. (1998) who reported that the absorption band of synthetic clinoenstatite at 9.9 μm (1010 cm^{-1}) did not shift with chemical composition. We also detected no shift within the compositional range measured by Jäger et al. (En$_{100}$ ~ En$_{70}$). However, in the Fe–rich compositional range (En$_{50}$ and Fs), shift towards the red was significant. In addition to the 9.9 μm band, double structured band at about 736 cm^{-1} (13.6 μm) does not shifted, *either*.

In contrast to the shift of most bands to the red with an increase in Fe concentration, two prominent bands at around 950 cm^{-1} and 875 cm^{-1} (10.7 μm and 11.7 μm in En$_{100}$) shift to significantly to shorter wavelength with increasing the iron concentration. For Mg–rich pyroxenes, incidental small bands and/or shoulders exist on the blue side of these bands, that is, at around 975 cm^{-1} (10.3 μm) and 900 cm^{-1} (11.1 μm). These four bands are separated on Mg–rich compositions. However, on Fe–rich compositions, these bands are degenerated to two bands. This band degeneration may be related to the reversed behaviour of peak shift.

3.3. Bandwidth variation with Mg/(Mg+Fe) ratio

In addition to the band shift, the variation of band width are observed especially in the sequence of the band shift from 40 to 56 micron (Table 3). It seems that the band width of both the Mg and the Fe end members are smaller than that of solid solutions. On the analogy of olivine (see Jäger et al. 1998), the vibrational modes of SiO$_4$–tetrahedra and divalent cation can be considered as the origin of the far-IR features. The broadening of the band width can be explained qualitatively with the overlap or unharmonicity of potentials of mixed phonon modes by Mg^{2+}–SiO$_4$ and Fe^{2+}–SiO$_4$.

In contrast, significant variation of band width in the mid-IR region are not detected. These results suggest that the
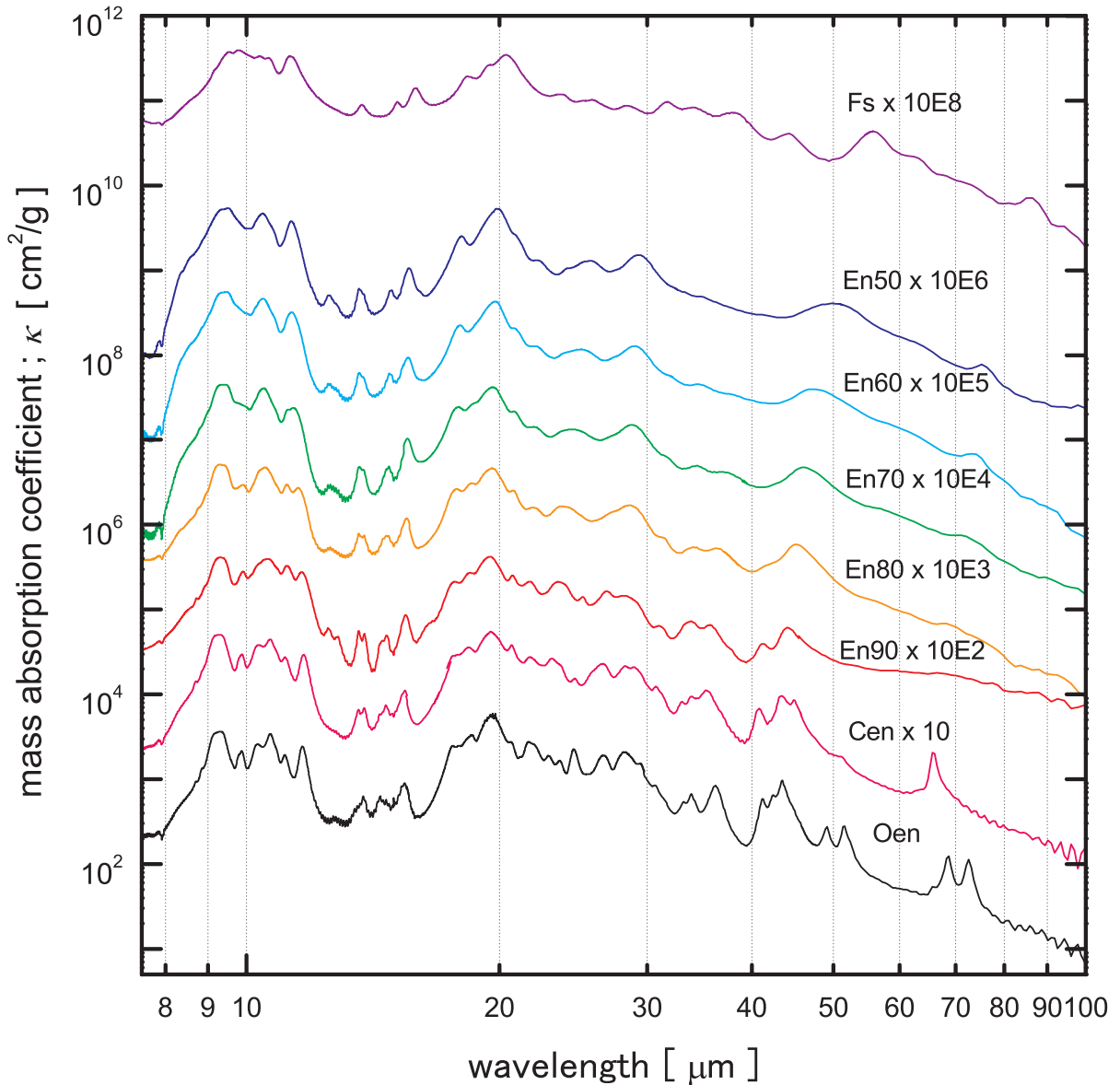
Fig. 1. The mass absorption coefficients, κ [cm^2/g], at room temperature. The Mg/(Mg+Fe) ratio decreases with the interval of every 10% from the bottom to top-ward (En$_{100}$–En$_{50}$). The spectra of the Mg end members are plotted at bottom. The uppermost one is for Fs.

far-infrared features are very sensitive to chemical composition and the crystal structure.

4. Discussion

Previously, from the ISO–SWS observations the main constituent of circumstellar pyroxenes was identified as orthoenstatite due to the existence of large 33 μm band similar to the laboratory band reported by Koike & Shibai (1998) (Waters et al. 1996). However, this absorption band was not detected so strongly by other works. Recently, Molster et al. (2002) also pointed out that the identification of orthoenstatite by this band should be reconsidered. However, we find that it is rather difficult to distinguish between ortho– and clinoenstatite in the ISO–SWS spectral range (wavelengths below 40 μm) because

the laboratory spectral features of ortho- and clinoenstatite are very similar in the mid-IR region.

In contrast, our new results suggest that the far-infrared features are much better indicators of the differences between ortho and clinoenstatite. In contrast to the discovery of the 69 μm band of olivine (e.g. Malfait et al. 1998, 1999; Molster et al. 2002; Bowey et al. 2001, etc.) the 70 micron double bands of orthoenstatite have not been reported, even for the objects in which the existence of orthoenstatite has been reported.

In geological environment, Mg–Fe pyroxene is usually orthorhombic in structure but in meteorites both ortho- and clinopyroxene are common. The phase diagram of Mg–Fe pyroxene at the atmospheric pressure shows that protoenstatite is stable at high temperature in the compositional range from En$_{100}$ to about En$_{80}$ (see Huebner 1980 for details of protoenstatite). This protoenstatite phase transforms to the monoclinic

Table 2. Peak positions in μm at room temperature. Prominent bands are indicated by bold face, and very small bands or shoulders are underlined. Values in brackets of En$_{90}$ are probably due to contamination of forsterite.

Oen	Cen	En$_{90}$	En$_{80}$	En$_{70}$	En$_{60}$	En$_{50}$	Fs
8.7	8.7	8.7					
8.9		8.9					
9.2	**9.2**	9.3	**9.3**	**9.3**	**9.3**	**9.3**	9.5
9.3	9.3	**9.4**	**9.4**	**9.5**	9.5	**9.5**	9.8
9.86	9.88	9.91	9.90	9.88		10.04	10.36
10.3	10.3	10.3	10.4				
10.7	**10.7**	**10.6**	**10.5**	**10.5**	**10.5**	**10.5**	
							10.6
11.1	11.1	11.2	11.2	11.2	**11.3**	**11.3**	**11.3**
11.7	**11.7**	11.6	11.5	11.4			
12.7		12.5	12.6	12.5	12.5	12.5	
		(12.9)					
	13.59	13.60	13.60	13.61	13.63	13.61	13.71
13.76	13.81	13.81	13.81	13.78	13.75	13.81	
14.4	14.4	14.5					
	14.6	14.7	14.8	14.8	14.8	14.9	15.1
15.4	**15.4**	**15.5**	**15.5**	**15.6**	**15.6**	**15.6**	15.9
		(16.5)					
17.6	17.6	17.7	17.8	17.9	18.0	18.0	18.3
							19.5
18.6	18.4	18.5	18.5	18.7			
19.5	**19.5**	**19.5**	**19.6**	**19.6**	**19.8**	**19.8**	**20.4**
20.7	20.7	20.7	20.8	20.8	20.9	20.8	
21.7	21.7	21.7	22.0	22.0	22.0	22.2	23.6
22.0							
22.9	23.1		23.8	23.8	23.9	24.1	25.2
23.6	23.6	23.5	24.3	24.4	25.0	25.7	25.8
							28.4
24.5	24.6	25.2					
26.6	26.6	26.9	27.2				
28.1	28.3	28.1	28.5	28.8	**29.0**	**29.3**	**31.7**
29.4	28.9						
30.7	30.7	31.0	31.4	31.7	32.2		
33.1	33.0						
							34.0
33.9	33.9	33.8	34.0	34.3	34.6	34.8	
							38.1
36.2	35.3	35.6	36.3	37.0			
41.2	**40.8**	41.2	41.6				
							44.3
42.4	43.4	**44.1**	**45.1**	**45.9**	**47.1**	**49.9**	**55.8**
							62.5
43.5	44.9						
49.2							
51.6							
	51.0						
	65.9						
			68.9	72.1	74.1	75.8	**86.1**
68.7							
72.5							

phase (clinoenstatite) as a metastable phase when it is cooled rapidly. Therefore, Mg–rich phases produced from melts at high temperature and quenched are monoclinic. In contrast, if protoenstatite is cooled very slowly or annealed at moderate temperature for long time, it transforms to the orthorhombic phase (orthoenstatite). Hence, if the crystal structure of circumstellar pyroxenes is determined by observations, we can give some more informations about condition of grain formations such as time scale of annealing and cooling and temperature of crystallization. For example, in the case that grain condensed close to photosphere, and then moves to outward along to stellar outflow, it is expected that clinopyroxenes will be produced since the grain will experience a steep temperature gradient. However, in the case that grain formation occurred slowly at
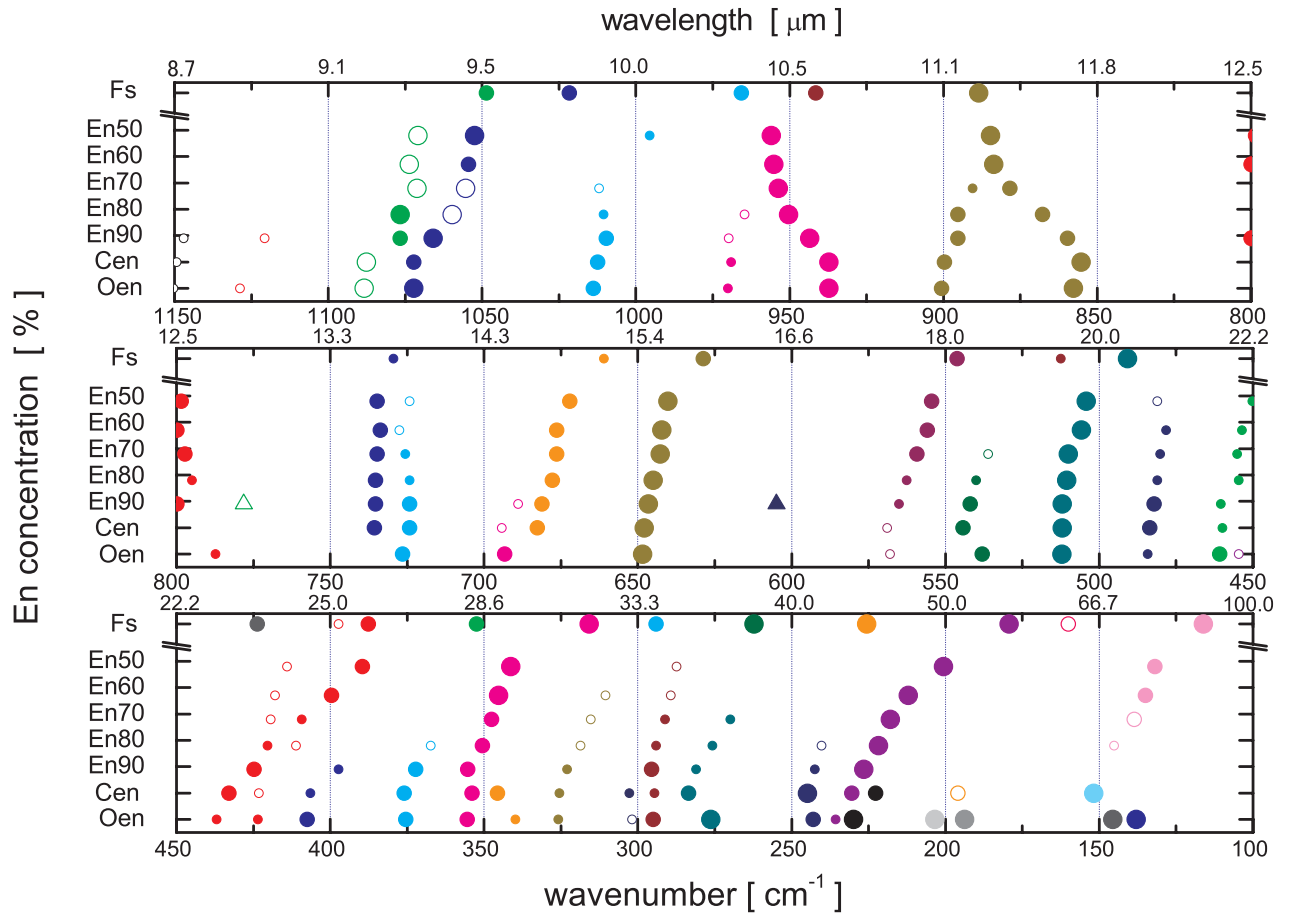
Fig. 2. Peak positions of absorption bands depending on chemical composition. Triangles plotted at 778 and 605 cm^{-1} on En$_{90}$ are probably due to contamination of forsterite.

Table 3. FWHM for 40-56 micron bands.

Sample	Peak Center [μm]	*FWHM* [μm]
En$_{90}$	44.1	3.1
En$_{80}$	45.1	4.6
En$_{70}$	45.9	5.4
En$_{60}$	47.1	6.1
En$_{50}$	49.9	7.8
Fs	55.8	5.6

moderate temperature, it is expected that orthopyroxenes are produced preferentially.

As mentioned previously, the far-IR absorption features are very sensitive to the chemical composition and crystal structure. Our results suggest that these chemical and physical properties of circumstellar pyroxene can be inferred from position, intensity and width of these absorption bands. To date, Fe–bearing or/and Fe–rich pyroxenes have not been identified in the ISO observations. From the results of this work, in the wavelength range of ISO–SWS, the degree of variations depending on the chemical composition is smaller than that in the far-IR region, and the characteristic far-IR features became broad with a moderate increase in iron content. Therefore, observational uncertainties such as signal to noise ratio and/or the

physical conditions in circumstellar regions (e.g. dust temperature) can mask compositional differences making the identification of the Fe–bearing pyroxenes difficult. In the present circumstance, in any case, since the iron concentration of the dust is estimated less than 10% at most, and if it is correct, further experimental investigation between En$_{100}$ and En$_{90}$ should be required.

In future when the precise observation in the far-IR region will have been available, the chemical and physical properties of circumstellar pyroxenes such as composition and crystal structure will be better determined by use of the far-IR characteristic features as a diagnostic maker.

References

Bowey, J. E., Lee, C., Tucker, C., et al. 2001, MNRAS, 325, 886
Chihara, H., Koike, C., & Tsuchiyama, A. 2001, PASJ, 53, 243
Huebner, J. S. 1980, in Rev. in Mineralogy, vol. 7, Pyroxenes, ed. C. T. Prewitt (Mineralogical Society of America), Ch. 5

Jäger, C., Molster, F. J., Dorschner, J., et al. 1998, A&A, 339, 904

Koike, C., Shibai, H., & Tsuchiyama, A. 1993, MNRAS, 2634, 654

Koike, C., & Shibai, H. 1998, ISAS Rep., No. 671

Koike, C., Tsuchiyama, A., Shibai, H., et al. 2000, A&A, 363, 1115

Malfait, K., Waelkens, C., Waters, L. B. F. M., et al. 1998, A&A, 332, L25

Malfait, K., Waelkens, C., Bouwman, J., et al. 1999, A&A, 345, 181

Molster, F. J., Waters, L. B. F. M., Tielens, A. G. G. M., et al. 2002, A&A, 382, 241-255

Rietmeijer, F. J. M., Nuth III, J. A., & Karner, J. M. 1999, ApJ, 527, 395

Tachibana, S. 2000, Ph.D. Thesis, Osaka University

Tielens, A. G. G. M., Waters, L. B. F. M., Molster, F. J., & Justtanont, K. 1997, Ap&SS, 255, 415

Waelkens, C., Waters, L. B. F. M., De Graauw, M. S., et al. 1996, A&A, 315, L245

Waters, L. B. F. M., Molster, F. J., de Jong, T., et al. 1996, A&A, 315, L361

Whittet, D. C. B., Schutte, W. A., Tielens, A. G. G. M., et al. 1996, A&A, 315, L357

Wood, B. J., Bryndzia, L. T., & Johnson, K. E. 1990, Science, 248, 337